Available online at www.derpharmachemica.com

ISSN 0975-413X
CODEN (USA): PCHHAX

Der Pharma Chemica, 2016, 8(2):22-35
(http://derpharmachemica.com/archive.html)

Electrochemical and DFT calculation studies on corrosion inhibition of 2-(2 Pyridyl) benzimidazole for C38 steel in hydrochloric acid solution

L. Afia[1], M. Larouj[2], H. Lgaz[1,2], R. Salghi[1*], S. Jodeh[3,*], S. Samhan[4] and M. Zougagh[5,6]

[1]*Laboratory of Applied Chemistry and Environment, ENSA, Université Ibn Zohr, Agadir, Morocco*
[2]*Laboratory separation processes, Faculty of Science, University Ibn Tofail, Kenitra, Morocco*
[3]*Department of Chemistry, An-Najah National University, Nablus, Palestine*
[4]*Palestine Water Authority, Ramallah, Palestine*
[5]*Regional Institute for Applied Chemistry Research, IRICA, E-13004, Ciudad Real, Spain*
[6]*Castilla-La Mancha Science and Technology Park, E-02006, Albacete, Spain*

ABSTRACT

The corrosion inhibition properties of 2-(2-Pyridyl) benzimidazole (PB) for C38 steel in HCl 1M solution were analysed by electrochemical impedance spectroscopy (EIS) and potentiodynamic polarization methods. The protection efficiency increases with increasing inhibitor concentration to attain 98.8 % at 2.10-4M. Potentiodynamic polarization data suggests mixed-mode of corrosion inhibition with predominant control of cathodic reaction. The studied inhibitor follows Langmuir adsorption isotherm. Data, obtained from EIS measurements, were analyzed to model the corrosion inhibition process through appropriate equivalent circuit model; a constant phase element (CPE) has been used. The effect of temperature on the corrosion behavior of C38 steel in 1 M HCl, with the addition of PB was also studied and it can be regarded as temperature-independent inhibitor. The activation energy as well as other thermodynamic parameters for the inhibition process was calculated and discussed. The results obtained showed that the PB could serve as an effective inhibitor of the corrosion of C38 steel in hydrochloric acid solution. Quantum chemical parameters were calculated using ab initio and DFT methods to find a good correlation with the inhibition efficiency. A good correlation was found between the theoretical calculations and experimental observations.

Keywords: Corrosion, Steel, Inhibition, 2-(2-Pyridyl) benzimidazole, HCl, Langmuir

---

INTRODUCTION

The corrosion is a main problem for steel industry, especially in acidic media. The inorganic acids are widely used in many processes such as pickling, cleaning and descaling therefore; corrosion prevention has critical importance [1–3]. Suitable method for corrosion protection in acid medium is addition of inhibitors. In the oil extraction and processing industries, inhibitors have always been considered the first line of defense against corrosion. Generally, the most efficient inhibitor molecules contain nitrogen, sulfur, oxygen, multiple bonds and aromatic rings [4–12]. The polar function is usually regarded as the reaction center for the establishment of the adsorption process [13]. Thus, the predominant mechanism of action of an inhibitor may vary with factors such as its concentration, pH, the nature of the anion, the presence of other species in the solution, the extent of reactions to form secondary inhibitors and the nature of the metals [14–18]. Basically, the adsorption process is constituted of two dependent steps; inhibitor molecules transfer from the bulk aqueous media to the double-layer and then adsorb onto the corroding surface; resulting in construction of a protective layer [19]. Therefore, hydrodynamic flow can be a vital environmental factor which influences on inhibitor performance by facilitating the molecular transport process from bulk solution to surface (positive effect), inducing a surface shear stress and promoting inhibitor desorption (negative effect). Thus, the adsorption of inhibitors may blocks either cathodic, anodic, or both reactions. In recent years, there is a considerable amount of effort devoted to develop novel and efficient corrosion inhibitors. Several works have

studied the influence of organic compounds on the corrosion of steel in acidic media such as azole [20-27], pyridine [28-33] sulfuric [34-37] and amino acid [38-41] compounds. Benzimidazole and its derivatives have received considerable attention on their inhibition properties for metallic corrosion over the past years [42–44]. Benzimidazole is a heterocyclic organic compound, the nitrogen atom and the aromatic ring in molecular structure are likely to facilitate the adsorption of the compounds on the metal surface [45]. Some derivatives of benzimidazole have been demonstrated as excellent inhibitors for metals and alloys in acidic solution, and exhibit different inhibition performance with the difference in substituent groups and substituent positions on the imidazole ring [46–52]. The 2-Amino-5-mercapto-1,3,4-thiadiazole [53], 2-amino-5-alkyl-1,3,4-thiadiazole [53–55], Schiff's base [56] and 2-amino-5-(n-pyridyl)-1,3,4-thiadiazole [57] and 2-(4-pyridyl)-benzimidazole [58] have been verified to be efficient inhibitors for steel in acidic media. Lagrenée group has synthesized series of 2, 5-disubstituted 1,3,5-thiadiazoles compounds, in which the substituted groups include pyridyl [59–62]. The 2-(2-Pyridyl) benzimidazole (PB) (Fig.1) used for the study was obtained from Sigma company –Aldrich (Germany).

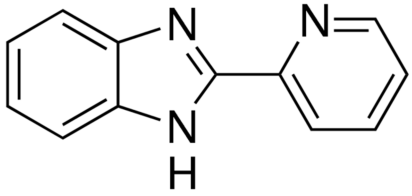

Fig. 1 Chemical structure of 2-(2-Pyridyl) benzimidazole

MATERIALS AND METHODS

2.1. Test solutions

HCl solutions were prepared by dilution of analytical commercial grade 37% HCl with deionised water. The inhibitor effect of PB was determined by electrochemical impedance spectroscopy EIS and potentiodynamic polarization techniques. The corrosion tests were performed in a 1M HCl solution in the absence of inhibitor and in the presence of a variety of concentrations of PB ranging from 10^{-6} M to 10^{-3} M. The electrochemical tests were carried out under air atmosphere with stirring the solutions. The temperature of the solutions was controlled thermostatically.

2.2. Electrochemical tests

The electrochemical study was carried out using a potentiostat PGZ100 piloted by Voltamaster software. This potentiostat is connected to a cell with three electrode thermostats with double wall (Tacussel Standard CEC/TH). A saturated calomel electrode (SCE) and platinum electrode were used as reference and auxiliary electrodes, respectively. The material used for constructing the working electrode was the same used for gravimetric measurements. The surface area exposed to the electrolyte is 0.56 cm^2. Potentiodynamic polarization curves were plotted at a polarization scan rate of 0.5 mV/s. Before all experiments, the potential was stabilized at free potential during 30 min. The polarisation curves are obtained from −700 mV to −300 mV at 298 K. The solution test is there after de-aerated by bubbling nitrogen. Gas bubbling is maintained prior and through the experiments. Electrochemical impedance spectroscopy (EIS) measurements are carried out with the electrochemical system (Tacussel), which included a digital potentiostat model Voltalab PGZ100 computer at E_{corr} after immersion in solution without bubbling. After the determination of steady-state current at a corrosion potential, sine wave voltage (10 mV) peak to peak, at frequencies between 100 kHz and 10 mHz are superimposed on the rest potential. Computer programs automatically controlled the measurements performed at rest potentials after 0.5 hour of exposure at 298 K. The impedance diagrams are given in the Nyquist representation. Experiments are repeated three times to ensure the reproducibility.

2.3. Quantum Chemical Study

Quantum chemical calculations are very effective methods for determining a correlation between molecular structure and inhibition efficiency. They can also be utilized to support the accuracy of experimental results [63–65]. Thus, it is important to compute the quantum chemical parameters, such as the energy of the highest occupied molecular orbital (EHOMO), the energy of the lowest unoccupied molecular orbital (ELUMO), the fraction of electrons transferred (ΔN) and the energies of the frontier molecular orbitals. In the present study, density functional theory (DFT) was used to determine the molecular structure of (PB) as a corrosion inhibitor for C38. The corrosion inhibition behavior of (PB) on the C38 in acidic solution was investigated using some experimental techniques. Quantum chemical computations were carried out by density function theory (DFT) with 6-31-G (d, p) basis set. All of the calculations were carried out with Gaussian 03W package [66, 67]. The following quantum chemical parameters were acquired: EHOMO, ELUMO, EHOMO - ELUMO energy gap (ΔE), electronegativity (χ), global

hardness (η), global softness (σ), fraction of electrons transferred (ΔN) and Mulliken charges on the backbone atoms.

RESULTS AND DISCUSSION

3.1. Electrochemical impedance spectroscopy measurements

Electrochemical impedance spectroscopy is a powerful tool for studying corrosion inhibition phenomena [68-70]. In order to get more information about the corrosion behavior of steel in 1M HCl, electrochemical impedance spectroscopy (EIS) measurements were obtained in the absence and presence of various concentrations of PB at 298 K and Nyquist plots were presented in Fig. 2. The electrochemical impedance parameters derived from this investigation are mentioned in Table 1.

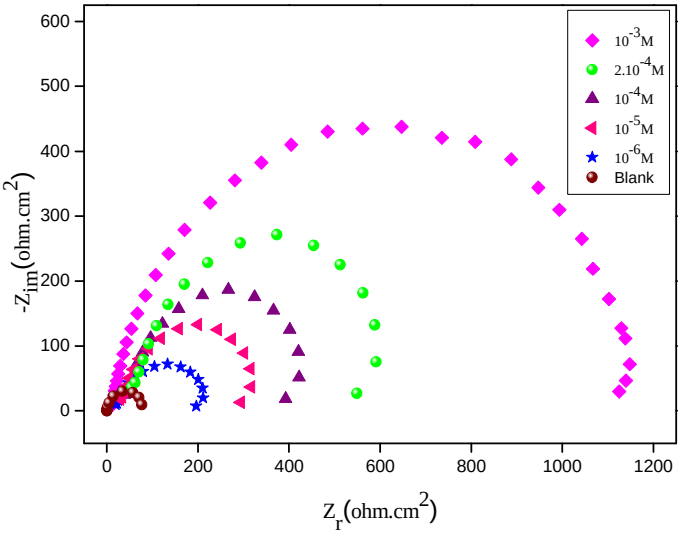

Fig. 2. Nyquist diagrams for C38 steel electrode with and PB at E_{corr}

The values of the polarization resistance were calculated by subtracting the high frequency intersection from the low frequency intersection [71]. Double layer capacitance values were obtained at maximum frequency (f_{max}), at which the imaginary component of the Nyquist plot is maximum, and calculated using the following equation:

$$C_{dl} = \frac{1}{2.\pi.f_m.R_t} \quad (1)$$

With C_{dl}: Double layer capacitance ($\mu F.cm^{-2}$); f_{max}: maximum frequency (Hz) and R_t: Charge transfer resistance ($\Omega.Cm^2$).

The inhibition efficiency can be calculated by the following formula:

$$E_{Rt}\% = \frac{(R_t - R^\circ_t)}{R_t} x100 \quad (2)$$

Were R_t and R^0_t are the charge transfer resistances in inhibited and uninhibited solutions respectively.

Table 1. Electrochemical Impedance parameters for corrosion of C38 steel in acid medium at various contents of PB.

Conc. (M)	R_t ($\Omega.cm^2$)	$10_{-5}A$ ($\Omega^{-1}S^n cm^2$)	N	f_{max} (Hz)	C_{dl} ($\mu F/cm^2$)	E_{RT} (%)
Blank	74	12.82	0.8984	75.72	75.72	-
10^{-6}	214	5.98	0.8732	41.34	32.77	65.4
10^{-5}	365	5.14	0.8698	29.95	25.25	79.7
10^{-4}	503	3.42	0.8624	21.39	16.05	85.3
2.10^{-4}	690	2.36	0.8423	14.04	12.46	89.3
10^{-3}	1170	1.98	0.8345	11.58	10.28	93.7

As shown in Fig. 2, all the impedance spectra exhibit one single capacitive loop, which indicates that the corrosion of steel is mainly controlled by the charge transfer process, and usually related to the charge transfer of the corrosion process and double layer behavior [72,73]. The capacitive loops are slightly depressed as semi-circular shapes because of the roughness and other inhomogeneities of C38 steel surface resulting in a phenomenon called ‘‘dispersing effect’’[74,75]. The diameters of those loops increase with increasing concentrations of PB. In addition, the shape is maintained throughout all tested inhibitor concentrations compared with that of blank solution. Thus, there is almost no change in the corrosion mechanism whether the inhibitor is added [76]. The nyquist’s plot of C38 steel in the absence of the inhibitor contains a slightly depressed semi-circular shape and only one time constant was seen as expected from literature [77, 78]. Accordingly, the EIS data are simulated by the equivalent circuit using ZWiev2 fitting program and it was given in fig.3. R_s and R_{ct} are the solution resistance and charge transfer resistance, respectively. CPE is constant phase element to replace a double layer capacitance (C_{dl}) for more accurate fit [79]. The impedance of a CPE is described by the expression:

$$Z_{CPE} = Y^{-1}(j\omega)^{-n} \quad (3)$$

Where Y is the magnitude of CPE, ω is the angular frequency ($2\pi f_{max}$), and the deviation parameter n is a valuable criterion of the nature of the metal surface and reflects microscopic fluctuations of the surface. For n = 0, Z_{CPE} represents a resistance with $R = Y^{-1}$; n = -1 an inductance with $L = Y^{-1}$, n = 1 an ideal capacitor with C = Y [80]. The idealized capacitance (C_{id}) values can be described by CPE parameter values Y and n using the following expression [81]:

$$C_{id} = Y\omega^{n-1}/\sin(n^{\pi/2}) \quad (4)$$

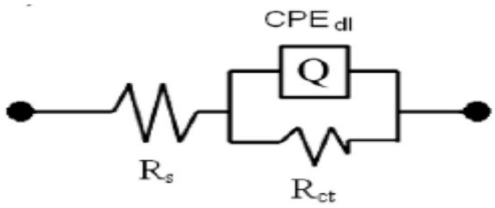

Fig. 3 The electrochemical equivalent circuit used to fit the impedance spectra

Figs. 4 and 5 correspond to the fitted plots for EIS experiment data using the electric circuit of Fig.3 in the absence and presence of 10^{-3}M of PB.

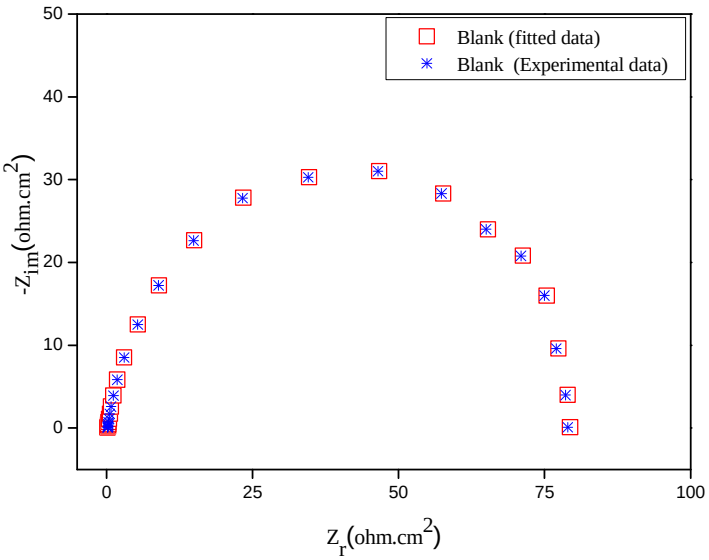

Fig. 4 EIS Nyquist plots for C38 steel in 1M HCl

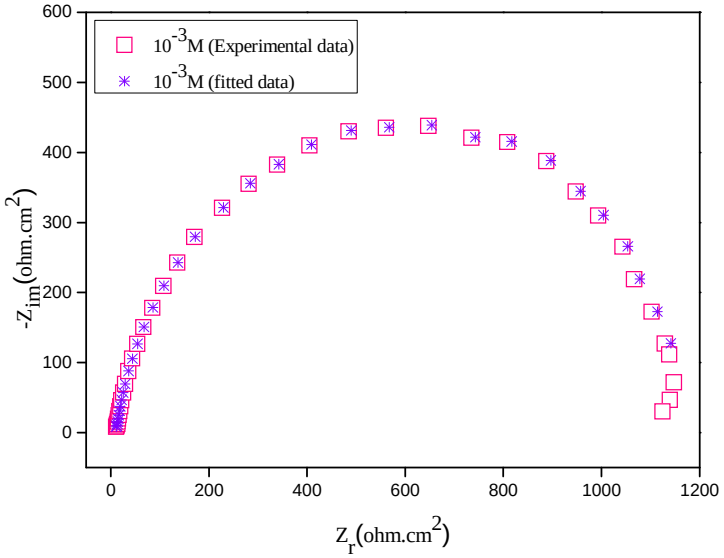

Fig. 5 EIS Nyquist plots for C38 steel in 1M HCl + 10^{-3}M of PB interface

Fig. 6 illustrates variation of Double layer capacitance (C_{dl}) and inhibition efficiency (E_{RT}) with PB compound concentration for steel in 1M HCl at 298 K. Excellent fit with this model was obtained with our experimental data (Figs. 4 and 5). It is observed that the fitted data match the experimental, with an average error of about 0.1%.

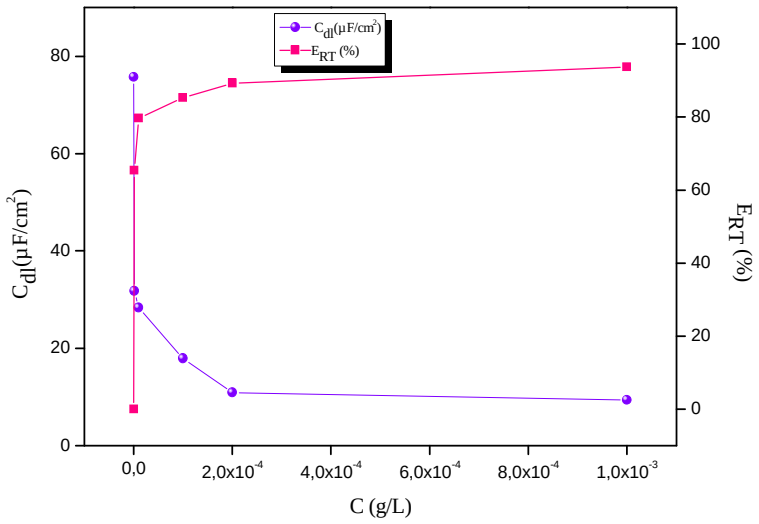

Fig. 6 Variation of Double layer capacitance (C_{dl}) and inhibition efficiency (E_{RT}) with PB compound concentration for steel in 1M HCl at 298 K

According to the equivalent circuit, the addition of PB to the corrosive solution increases the charge transfer resistance (R_t) and decreases the double layer capacitance (C_{dl}). Kosari et al. [82] studied other pyridine derivatives, which were pyridine-2-thiol (P2T) and 2-pyridyl disulfide (2PD), against corrosion of steel in HCl medium. In their research, the R_t values of steel electrode in 200 ppm P2T and 2PD containing 0.1 M HCl solutions were 918 and 701 Ω. cm^2, respectively. The double layer between the charged metal surface and the solution is considered as an electrical capacitor. The decrease of capacity in inhibited system may be attributed to the formation of a protective layer on the electrode surface [83]. The decreased C_{dl} values can result from the increase of thickness of electrical double layer or decrease of the local dielectric constant which suggest the substitution of H_2O molecules (with higher dielectric constant) with inhibitor molecules (with lower dielectric constant) leading to a protective film on electrode surface [84]. Generally, the deviation of *n* from the values of 1 can be considered as a measure of the surface inhomogeneity [85, 86] and the efficiency reaches 93.7% at 10^{-3}M of PB.

3.2. Polarization curves

Potentiodynamic polarisation curves of C38 steel in 1M HCl in the absence and presence of PB at different concentrations at 298 K are presented in Fig.7. The corrosion parameters including corrosion current densities (I_{corr}), corrosion potential (E_{corr}), cathodic Tafel slope (β_c) and inhibition efficiency (E_I %) are listed in Table 2.

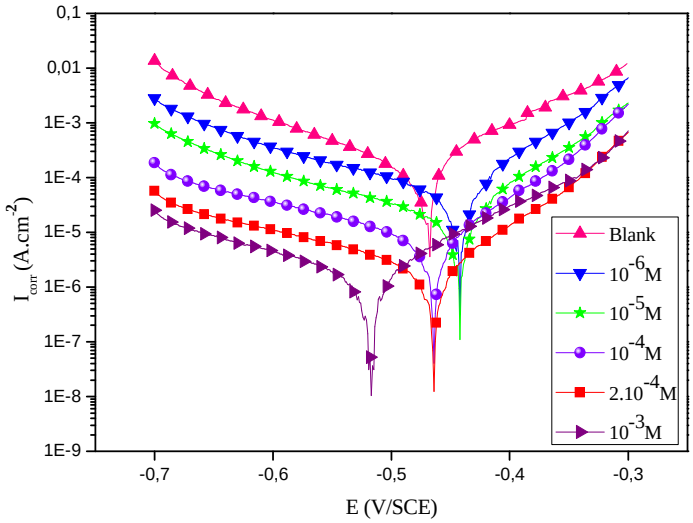

Fig. 7 Potentiodynamic polarisation curves of C38 steel in 1M HCl in the presence of different concentrations of PB

Table 2 Electrochemical parameters of C38 steel at various concentrations of PB in 1M HCl and corresponding inhibition efficiency

Concentration (M)	E_{corr} (mV/SCE)	I_{corr} ($\mu A/cm^2$)	$-b_c$ (mV/dec)	E_I (%)
Blank	-567	114.0	123	-
10^{-6}	-442	43.7	128	61.7
10^{-5}	-442	16.0	130	86.0
10^{-4}	-464	7.1	133	93.8
2.10^{-4}	-464	2.3	127	98.0
10^{-3}	-516	1.4	125	98.8

In this case, the inhibition efficiency is defined as follows:

$$E\% = (1 - \frac{I'_{corr}}{I_{corr}})x100 \quad (7)$$

Where I_{corr} and I'_{corr} are current density in absence and presence of PB respectively. We noted that I_{corr} and I'_{corr} were calculated from the intersection of cathodic and anodic Tafel lines. It is clear from Fig. 7 that, as the inhibitor is added to the corrosive medium both anodic dissolution of iron and cathodic hydrogen evolution reactions were retarded. The inhibitions of these reactions are more pronounced with the increasing inhibitor concentration while the corrosion potential values shifted the more negative values, which prove that the inhibitor affects the cathodic reaction more than the anodic reaction. These results indicate that PB acts as the mixed type corrosion inhibitor with predominant control of the cathodic reaction. The cathodic current–potential curves are giving rise to parallel lines. This indicates that the addition of PB to the 1 M HCl solution does not change the hydrogen evolution mechanism. The reduction of H^+ ions at the C38 steel surface take place mainly through a charge transfer mechanism [87–89]. The inhibitor molecules are first adsorbed onto the C38 steel surface and, therefore, impedes by merely blocking the reaction sites of the steel surface. As revealed by the data presented in Table 2, it is evident that the corrosion current density (I_{corr}) of the C38 steel is much smaller when PB is added to the aggressive solution. Correspondingly, E_I % values increase with increasing the inhibitor concentration reaching a maximum value 98.8% at 10^{-3}M of inhibitor. The increased inhibition efficiency with the inhibitor concentration indicates that the tested organic compound acts by adsorbing on the C38 steel surface [90]. The inhibition effect of the inhibitor may be caused by the simple blocking effect, namely the reduction of reaction area on the corroding surface [91–93]. Further, the values of the cathodic Tafel slope (β_c) in the presence of the inhibitor are not significantly changed with the inhibitor concentration. The inhibition efficiencies, calculated from impedance results, show the similar trend to those obtained from potentiodynamic polarization measurements. Also the inhibition ability of PB is confirmed by the impedance measurements.

3.3. Adsorption isotherm

The type of the adsorption isotherm can provide additional information about the properties of the tested compound. In order to obtain the adsorption isotherm, the degree of surface coverage (θ) of the inhibitor must be calculated. The experimental results were fitted to a series of adsorption isotherms, and the best fit was obtained with the use of the Langmuir adsorption isotherm, a straight line is obtained upon plotting C_{inh}/θ vs. C_{inh}, which is presented graphically in Fig. 8.

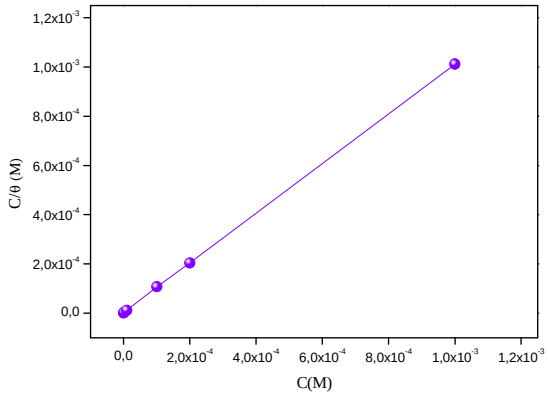

Fig. 8 Plot of Langmuir adsorption isotherm of PB on the steel surface at 298K

The relationship between surface coverage ratio, θ, and inhibitor absorption in the corrosive media can be represented as: [94]:

$$\frac{C}{\theta} = \frac{1}{K} + C \qquad (8)$$

Where C is the PB concentration, θ the fraction of the surface covered determined by E/100 from EI data, k the equilibrium constant for the adsorption–desorption process, which is related to the standard free energy of adsorption ΔG_{ads}, according to Eq 9, R is the universal gas constant, T is the thermodynamic temperature and the value of 55.5 is the concentration of water in the solution in mol/L.

$$\Delta G_{ads} = -RT(\ln 55.5K) \qquad (9)$$

The adsorption of organic molecules at the metal/solution interface consists of the replacement of water molecules by organic molecules according to following process [93]:

$$Org_{(sol)} + x\ H_2O_{(ads)} \longleftrightarrow Org_{(ads)} + x\ H_2O_{(sol)}$$

Where $Org_{(sol)}$ and $Org_{(ads)}$ are organic molecules in the solution and adsorbed on the metal surface, respectively, and x is the number of water molecules replaced by the organic molecules. The inhibitory efficiencies of the organic molecules mainly depend on their adsorption ability on the metal surface. Therefore, the determination of relation between adsorption and corrosion inhibition is of great importance. The correlation coefficients (0.9999) and the slopes (1.0109) are close to 1 which confirms this assumption. Therefore, it is concluded that, a monolayer inhibitor film forms on C38 steel surface, and there are no interactions between the adsorbed inhibitor molecules [95- 98]. The K value of $5.4226.10^5$ M^{-1} demonstrates that the PB compound highly adsorbs onto the surface of the C38 steel [98–103].

In general, if ΔG_{ads} values are around -20 kJ mol^{-1} or less negative is associated with an electrostatic interaction between charged inhibitor molecules and charged electrode surface, physisorption; those of -40 kJ mol^{-1} or more negative involve charge sharing or transfer from the inhibitor molecules to the metal surface to form coordinate type bond chemisorptions [104]. The calculated value of ΔG_{ads} for studied inhibitor is -11.22 kJ mol^{-1}; probably means that physical adsorption would take place.

3.4. Effect of temperature

Temperature has a great effect on the corrosion phenomenon. Generally In acidic media, dissolution of metal is generally accompanied with evolution of hydrogen gas and rise in temperature usually accelerates the corrosion

reactions, resulting in higher dissolution of metal. For this purpose, we made potentiostatic polarization in the range of temperature 298 to 328 K, in the absence and presence of PB at 2.10^{-4}M. The corresponding data are shown in fig 9, 10 and Table 3.

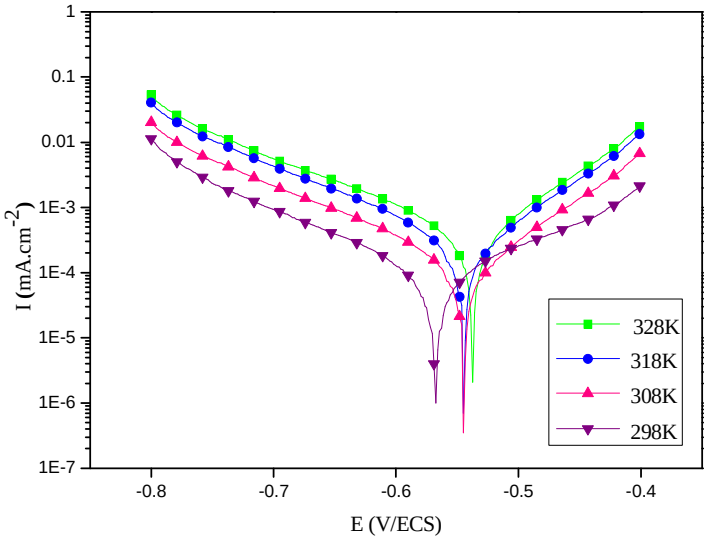

Fig. 9 Polarisation curves of C38 steel in 1M HCl

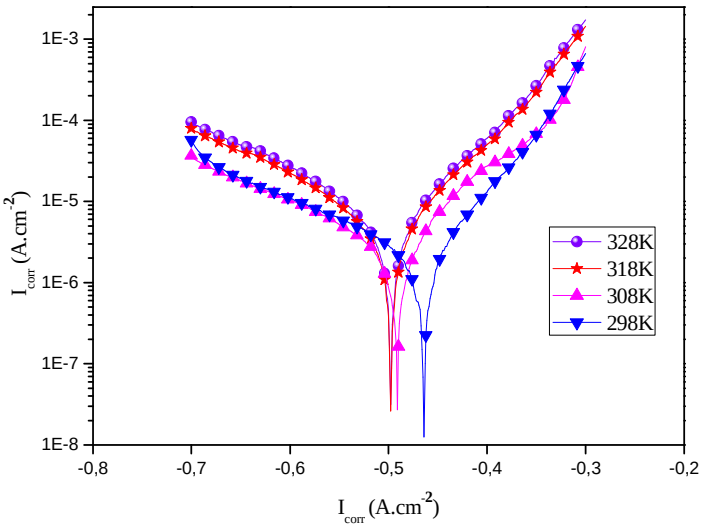

Fig. 10 Polarisation curves of C38 steel in 1M HCl in the presence of 2.10^{-4} M of PB at different temperatures

Table 3 Effect of temperature on the steel corrosion in the absence and presence of PB at2.10^{-4} M

Inhibitor	Temperature	E_{corr} (mV/SCE)	I_{corr} ($\mu A/cm^2$)	$-b_c$ (mV/dec)	E_I (%)
Blank	298	-567	114	123	-
	308	-544	157	126	-
	318	-545	305	129	-
	328	-537	399	136	-
PB	298	-464	2.3	127	98.0
	308	-491	2.9	104	98.2
	318	-497	2	177	99.3
	328	-498	4.5	169	98.9

As seen from Fig. 9 and 10 and Table 3, the corrosion current density increases with increasing temperature in uninhibited solutions. Slight changes in values of inhibition efficiencies are observed in the range of temperature studied. Thus the PB can be regarded as temperature-independent inhibitor. The nearly constant efficiency of the inhibitor in the temperature range studied can be considered as the slight change in the nature of the adsorption mode: physisorption of the inhibitor is dominant in the temperature range studied, while chemisorption accompanied by physisorption can occur slightly with increasing the temperature.

3.5. Kinetic parameters

In order to obtain more details on the corrosion process, activation kinetic parameters such as activation energies in free and inhibited acid were calculated using Arrhenius equation:

$$I_{corr} = A\exp(-\frac{Ea}{R.T}) \quad (10)$$

Where A is Arrhenius factor, E_a is the apparent activation corrosion energy, R is the perfect gas constant and T the absolute temperature.

Plotting (log I_{corr}) versus 1/T gives straight lines as revealed from Fig.11.

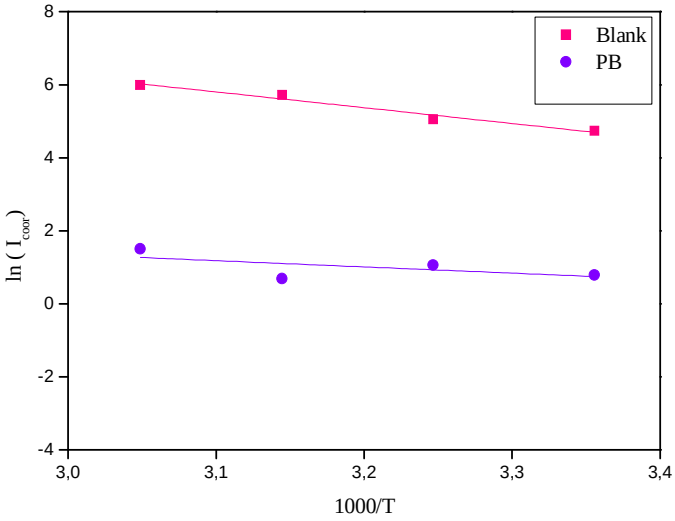

Fig .11 Arrhenius plots of steel in 1 M HCl with and without 2.10^{-4} M of PB

The activation energy values obtained are 14.13 and 35.90 kJ/mol for 2.10^{-4}M of PB and free acid, respectively. Notably, the energy barrier of the corrosion reaction decreased in the presence of the inhibitor. The lower value of the activation energy of the corrosion process in the presence of inhibitor compared to that in its absence is attributed to the existence of chemical process in the adsorption of inhibitor on steel surface [105]. The decrease of E_a value can be interpreted as slow rate of inhibitor adsorption with a resultant closer approach to equilibrium during the experiments at high temperature [106]. Behpour et al. [107] explained

the change of the activation energy from energetic heterogeneity of the surface as follows. Assuming that energetic surface is heterogeneous, active centers of the surface have different energy. Two possibilities may exist: in the first case, the inhibitor is adsorbed on the most active adsorption sites (having the lowest energy) and the corrosion process takes place predominantly on the active sites of higher energy, which results in the higher activation energy. In the second case, a smaller number of more active sites remain uncovered which take part in the corrosion process, resulting in the lower activation energy. However, Vracˇar and Drazˇic [108] argued that the criteria, adsorption type obtained from the change of activation energy, cannot be taken as decisive due to competitive adsorption with water whose removal from the surface requires also some activation energy. On the other words, the so-called chemisorption process may contain physical process simultaneously and vice versa.

Kinetic parameters, such as enthalpy and entropy of corrosion process, may be evaluated from the effect of temperature. An alternative formulation of Arrhenius equation is (11) [109]:

$$I_{corr} = \frac{RT}{Nh}.\exp(\frac{\Delta S^*}{R}).\exp(-\frac{\Delta H^*}{RT}) \quad (11)$$

Where N is the Avogadro's number, h the Plank's constant, R is the perfect gas constant, ΔS* and ΔH*the entropy and enthalpy of activation, respectively.

Fig. 12 shows a plot of ln (W/T) against 1/T for PB. Straight lines are obtained with a slope of (-ΔH*/R) and an intercept of (ln R/Nh + ΔS*/R) from which the values of ΔH*and ΔS* are calculated respectively (Table 4).

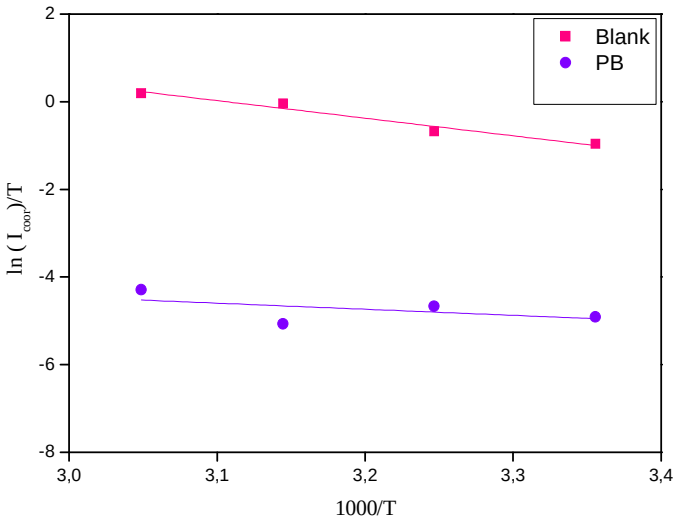

Fig.12 Relation between ln (W_{corr}/T) and 1000/T in acid at different temperatures

The value of free energy ΔG* is deduced from the formula (12):

$$\Delta G^* = \Delta H^* - T\Delta S^* \quad (12)$$

Table 4 The values of activation parameters ΔH*, ΔS*and ΔG* for C38 in 1M HCl in the absence and the presence of 2.10^{-4} M of PB

Inhibitor	ΔH* (kJ/mole)	ΔS* (J/mole^{-1}.k^{-1})	ΔG* (kJ/mole à T=298K)	Ea-ΔH*
Blank	33.32	-184.99	55.16	2.58
PB	11.47	-197.72	70.39	2.66

The values of E_a and ΔH*are close to each other as expected from the concept of transition state theory and vary in the same manner on the addition of inhibitor.

The positive sign of ΔH has been attributed to the endothermic nature of the C38 steel dissolution process [110-112].

The higher values of ΔS for inhibited solutions can be attributed to the increase in solvent entropy [111, 113–115]. However, C38 steel corrosion in the free acid was characterized by the more negative ΔS* value which implies that the activation complex in the rate determining step required association rather than dissociation [116].

The ΔG value for inhibited systems were more positive than that for the uninhibited systems revealing that in presence of inhibitor , the activated corrosion complex becomes less stable as compared to its absence.

3.6. Molecular structure and quantum chemical calculation

Quantum chemical calculations are utilized to ascertain whether there is a clear relationship between the molecular structure of the synthesized inhibitor and its inhibition effect. The structure parameters of the synthesized inhibitor are used to elucidate the inhibition mechanism in the present work. The optimized geometry and localization of the frontier molecular orbital on the PB structure are shown in Fig.13 and the quantum chemical parameters are listed in Table 5.

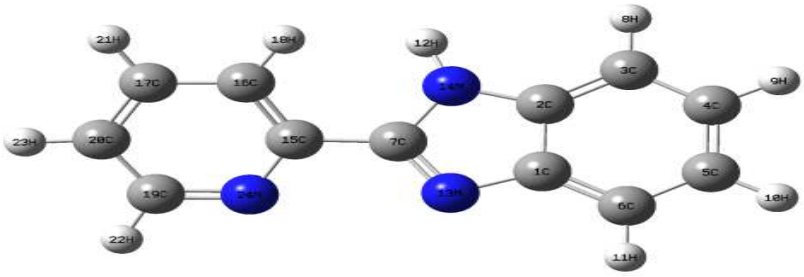

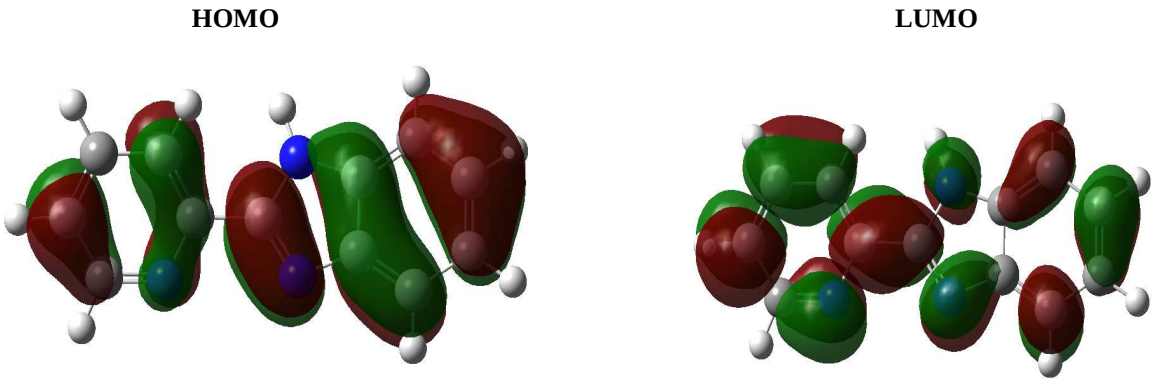

Fig. 13. Optimized geometry Frontier molecule orbital density distributions of the synthesized inhibitor

Analysis of Fig.13 shows that the distribution of two energies HOMO and LUMO, we can see that the electron density of the HOMO and LUMO location was distributed almost of the entire molecule. As per the frontier molecular orbital theory of chemical reactivity, transition of electrons occurs on interaction between the frontier-orbital that are HOMO and LUMO of the reacting species. The energy of HOMO characterizes the susceptibility of the molecule toward attack by electrophile and is related to the ionization potential. High value of E_{HOMO}

(-5.8807eV) probably indicates a tendency of the molecule (PB) to donate electrons to appropriate acceptor molecules with low energy and empty molecular orbital.whereas the energy of LUMO characterizes the susceptibility of the molecule toward attack by nucleophile and is related to the electron affinity. The electron accepting ability of the molecule (PB) increases with lower the values of E_{LUMO} (-1.3872eV). Smaller the energy gap between LUMO and HOMO, higher is the efficiency of inhibitor. The values of ΔE in Table 5, suggesting the strongest ability of the synthesized inhibitor to form coordinate bonds with d-orbitals of metal through donating and accepting electrons, is in good agreement with the experimental results. Additionally, for the dipole moment (μ), higher value of μ will favor the enhancement of corrosion inhibition [117]. From Table 5, the value of μ is higher, which is also in agreement with the experimental results mentioned above.

Table 5 Calculated quantum chemical parameters of the studied compound using (DFT) with 6-31-G (d, p) basis set

Molecule	E_{HOMO} (eV)	E_{LUMO} (eV)	ΔE (eV)	M (eV)	TE (eV)	H (eV)	σ (eV^{-1})	X (eV)	ΔN	IE (%)
PB	-5.8807	-1.3872	4.4935	4.8205	-17061	2.2468	0.4451	3.6339	0.749	93.7

Another method to correlate inhibition efficiency with parameters of molecular structure is to calculate the fraction of electrons transferred from inhibitor to metal surface. According to Koopman's theorem [118], E_{HOMO} and E_{LUMO} of the inhibitor molecule are related to the ionization potential (I) and the electron affinity (A), respectively. The ionization potential (I) and the electron affinity (A) are defined as follows:

$$I = -E_{HOMO} \quad (13)$$

$$A = -E_{LUMO} \quad (14)$$

Then absolute electronegativity (χ) and global hardness (η) of the inhibitor molecule are approximated as follows [119]:

$$\chi = \frac{I + A}{2} \quad (15)$$

$$\eta = \frac{I - A}{2} \quad (16)$$

Thus the fraction of electrons transferred from the inhibitor to metallic surface, ΔN, is given by [120]:

$$\Delta N = \frac{\chi_{Fe} - \chi_{inh}}{2(\eta_{Fe} + \eta_{inh})} \quad (17)$$

To calculate the fraction of electrons transferred the theoretical values of of χ_{Fe} (7 eV mol^{-1}) and of η_{Fe} (0 eV mol^{-1}) are used [121]. The calculated results are presented in Table 5. Value of ΔN show inhibition effect resulted from

electrons donation. According to Lukovits's study [122]. If ΔN < 3.6, the inhibition efficiency increases with increasing electron-donating ability at the metal surface. Based on these calculations, it is expected that the synthesized inhibitor is donor of electrons, and the steel surface is the acceptor. The Mullikan charge populations and the direction of dipole moment calculated for the three Schiff bases are projected to the molecular plane. The charge population and direction of the dipole moment can be understood by considering the electrostatic potential (middle and right panels of Fig. 14), which discerns electron density rich regions centered on nitrogen atoms in aromatic ring in molecular structure atoms and some of carbon atoms of aromatic rings. The regions of highest electron density are generally the sites to which electrophiles attacked [123]. So N and C atoms are the active center, respectively, which have the strongest ability of bonding to the metal surface.

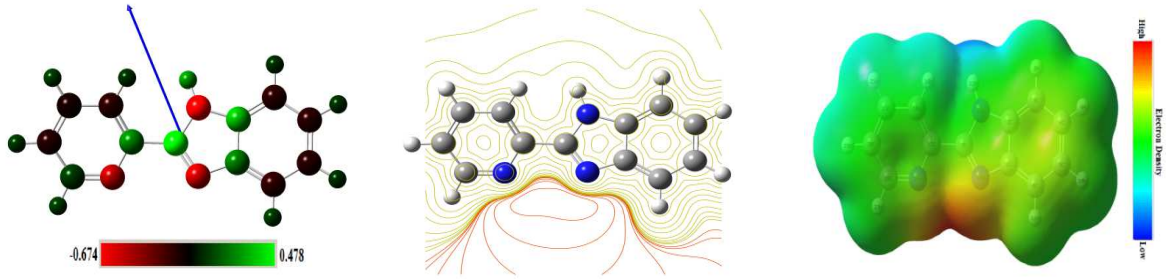

Fig.14 Electrostatic properties of (PB) side views of the dipole and the Mulliken charge populations are displayed on the left while the middle and right panels show the contour and isosurface representation of electrostatic potential respectively (the electron rich region is red and the electron poor region is blue)

CONCLUSION

From the above results and discussion, the following conclusions are drawn:
* The results showed that inhibitor 2-(2-Pyridyl) benzimidazole (PB) have excellent inhibition efficiency for the corrosion of C38 steel in 1 M HCl.
* The inhibition efficiency increases with concentration compound.
* The potentiodynamic polarization curves indicated that 2-(2-Pyridyl) benzimidazole act as mixed type of inhibitor.
* The 2-(2-Pyridyl) benzimidazole molecule follows Langmuir adsorption isotherm for the adsorption on metal surface in 1 M HCl solution.
* The impedance results indicate that the value of polarization resistance increased and double layer capacitance decreased. This result can be attributed to the increase of thickness of electrical double layer.
* Quantum chemical calculations showed a good correlation between quantum chemical parameters for the investigated compound and its inhibition efficiency for the corrosion process in agreement with experimental results.

Acknowledgment
The authors would like to thank MENA NWC for their financial support for grant no: WIF 04. Also, we would like to extend our thanks to Palestine Water Authority (PWA) and MEDRIC for their support. The support given through an "INCRECYT" research contract to M. Zougagh is also acknowledged.

REFERENCES

[1] Deng S, Li X, *Corros Sci* **2012**, 55, 407.
[2] Wang X, Yang H, Wang F, *Corros Sci* **2012**, 55,145.
[3] Solmaz R, Altunbas E, Kardas G, *Mater Chem Phys* **2011**, 125, 796.
[4] Cornua M, Koltsov A, Nicolas S, Colom L, Dossot M, *Appl Surf Sci* **2014**, 293**,** 24.
[5] Hegazy M A, El-Tabei A S, Bedair A H, Sadeq M A, *Corros Sci* **2012**, 54, 219.
[6] Hegazy M A, Abdallah M, Awad M K, Rezk M, *Corros Sci* **2014**, 81, 54.
[7] Sherif E M, *Appl Surf Sci* **2014**, 292, 104.
[8] Dogru Mert B, Mert M E, Kardas G, Yazıcı B, *Corros Sci.* **2011**, 53, 4265.
[9] Kowsari E, Payami M, Amini R, Ramezanzadeh B, Javanbakht M, *Appl Surf Sci.* **2014**, 289**,** 478.
[10] Torres V V, Rayol V A, Magalhaes M, Viana G M, Aguiar L C S, Machado S P, Orofino H, D'Elia E, *Corros Sci.* **2014**, 79, 108.
[11] Banerjee S, Srivastava V, Singh M M, *Corros Sci.* **2012**, 59, 35.
[12] Souza F S, Spinelli A, *Corros Sci* **2009**, 51, 642.

[13] Roberge P R, McGraw-Hill, New York, **1999**.
[14] Zhuk N P, Metallurgia, Moscow, **1976**.
[15] Schmitt G, Europhed. Of Corrosion, Dehema, Frankfurt/Main, **1988**.
[16] Roberge P R, Handbook of Corrosion Engineering, McGraw-Hill, NY, **2000.**
[17] Ivanov E S, Inhibitors for Metal Corrosion in Acid Media (Russ.), Metallurgy, Moscow, **1986**.
[18] Rosenfeld I L, Khimiya, Moscow, **1977**.
[19] Sastri V, John Wiley & Sons, Inc., Hoboken, New Jersey, **2011**.
[20] Ahmad Y H, Walid M I H, *Int. J. Electrochem. Sci.* **2012**, 7, 12456.
[21] Espinoza-Vázquez A, Negrón-Silva G E, Angeles-Beltrán D, Herrera-Hernández H, Romero Romo M, Palomar-Pardavé M, *Int. J. Electrochem. Sci*., **2014**, 9, 493.
[22] Deng Q, Ding N N, Wei X L, Cai L, He X P, Long Y T, Chen G R, Chen K X, *Corros. Sci*. **2012**, 64, 64.
[23] Tourabi M, Nohair K, Traisnel M, Jama C, Bentiss F, *Corros. Sci.* **2013**, 75, 123.
[24] Markhali B P, Naderi R, Mahdavian M, Sayebani M, Arman SY, *Corros. Sci*. **2013**, 75 269.
[25] Fouda A S, Ellithy A S, *Corros. Sci*. **2009,** 51, 868.
[26] Ongun Yuce A, ak Dog˘ru Mert B, Kardas G, Yazıcı B, *Corros. Sci*, **2014**, 85, 215.
[27] Obot B, Ebenso E, Kabanda M, *J. Environ .Chem. Engineer*, **2013**,1 , 431.
[28] Dog˘ru Mert B, Ongun Yuce A, Kardas G, Yazıcı B, *Corros. Sci*, **2014**, 85, 287.
[29] Lashkari M, Arshadi M R, *Chem. Phys*. **2004**, 299, 131.
[30] Kosari A, Moayed M H, Davoodi A, Parvizi R, Momeni M, Eshghi H, Moradi H, *Corros. Sc.*, **2014**, 78, 138.
[31] Lashkari M, Arshadi M R, *Chem Phys* **2004**, 299, 131.
[32] Kosari A, Moayed M H, Davoodi A, Parvizi R, Momeni M, Eshghi H, Moradi H, *Corros Sc* **2014**, 78, 138.
[33] Ergun U, Yuzer D, Emregul K C, *Mater. Chem. Phys*. **2008**, 109, 492.
[34] Torres V V, Rayol V A, Magalhães M, Viana G M, Aguiar L C S, Machado S P, Orofino H, D'Elia E, *Corros Sci* **2014**, 79, 108.
[35] Anejjar A, Salghi R, Zarrouk A, Benali O, Zarrok H, Hammouti B, Ebenso E E, *J Assoc Arab Univ Basic Appl Sci* **2014**, 15, 21.
[36] Daoud D, Douadi T, Issaadi S, Chafaa S, *Corros Sci* **2014**,79, 50.
[37] Doner A, Ongun Yuce A, Kardas G, *Ind Eng Chem Res* **2013**, 52 , 9709.
[38] Yuce A, Mert B, Kardas G, Yazıcı B, *Corros Sci* **2014**, 83**,** 310.
[39] Solmaz R, *Corros Sci* **79** (2014) 169.
[40] Zaafarany I A, *Int J Electrochem Sci* **2013**, 8.
[41] Doner A, Kardas G, *Corros Sci* **2011**, 53, 4223.
[42] Wang L, *Corros. Sci*. **2001**, 43, 2281.
[43] Popova A, Christov M, Deligeorgiev T, *Corros. Sci*. **2003**, 59, 756.
[44] Khaled K F, *Electrochim. Acta*. **2003**, 48, 2493.
[45] Wang W, Yang H, Wang F, *Corros. Sci*. **2011**, 53, 113.
[46] Popova A, Sokolova E, Raicheva S, Christov M, *Corros. Sci.* **2003**, 45, 33.
[47] Popova A, Christov M, Raicheva S, Sokolova E, *Corros.Sci*. **2004**, 46, 1333.
[48] Christov M, Popova A, *Corros. Sci*. **2004**, 46**,** 1613.
[49] Popova A, Christov M, Zwetanova A, *Corros. Sci*. **2007**, 49, 2131.
[50] Popova A, Christov M, Vasilev A, *Corros. Sci.* **2007**, 49, 3290.
[51] Ahamad I, Quraishi M A, *Corros. Sci*. **2010**, 52, 651.
[52] Ahamad I, Quraishi M A, *Corros. Sci*. **2009**, 51, 2006.
[53] Solmaz R, Kardas G, Yazici B, Erbil M, *Colloids Surf. A Physicochem. Eng. Aspects*. **2008**, 312, 7.
[54] Sherif E M, Park S, *Corros. Sci*. **2006**, 48, 4065.
[55] Zhou J, Chen S, Zhang L, Feng Y, Zhai H, *J. Electroanal. Chem*. **2008**, 612, 257.
[56] Ansari K R, Quraishi M A, Ambrish S, *Corros. Sci.* **2014**, 79, 5.
[57] Yongming T , Xiaoyuan Y, Wenzhong Y, Rong W, Yizhong C, XiaoshuangY , *Corros. Sci*. **2010**, 52, 1801.
[58] Zhang F, Tang Y M, Cao Z, Jing W H, Wu Z L, Chen Y Z. *Corros .Sci.* **2012**, 61,61.
[59] Azhar M E, Mernari B, Traisnel M, Gengembre L, Bentiss F, Lagrenee M, *Corros. Sci*. **2001**, 43, 2229.
[60] Lebrini M, Bentiss F, Vezin H, Lagrenee M, *Corros. Sci.* **2006**, 48, 1279.
[61] Bentiss F, Lebrini M, Vezin H, Lagrenee M, *Mater. Chem. Phys*. **2004**, 87, 18.
[62] Bentiss F, Traisnel M, Lagrenee M, *J. Appl. Electrochem*. **2001**, 31, 41.
[63] Doner A, Solmaz R, Ozcan M, Kardas G, *Corros. Sci*. **2011**, 53, 2902–2913.
[64] Obot I B, Gasem Z M, *Corros. Sci*. **2014**, 83, 359.
[65] Li. X, Deng S, Fu H, Xie X, *Corros. Sci*. **2014**, 78, 29.
[66] Frisch M J, Trucks G W, Schlegel H B, Scuseria G E, Robb M A, Cheeseman J R Jr.Gaussian03, revision E.01.Walling ford, CT: Gaussian Inc. (**2007**).
[67] Gauss View, Version 3.0, Gaussian Inc., Pittsburgh, PA, **2003**.
[68] Hermas A A, Morad M S, Wahdan M H, *J. Appl. Electrochem*. **2004**, 34, 95.

[69] Lorenz W J, Mansfeld F, *Corros. Sci*. **1981**, 21, 647.
[70] Popova A, Christov M, *Corros. Sci*. **2006**, 48, 3208.
[71] Ouachikh O, Bouyanzer A, Bouklah M, Desjobert J M, Costa J, Hammouti B, Majidi L, *Surf. Rev.Lett*, **2009**, 16, 49.
[72] Cao C N, Zhang J Q, *Corros Sci.* Press, **2002**, 172.
[73] Behpour M, Ghoreishi S M, Mohammadi N, Soltani N, Salavati-Niasari M, *Corros. Sci*. **2010**, **52**, 4046.
[74] Ramesh S, Rajeswari S, *Electrochim. Acta* . **2004**, 49, 811.
[75] Achouri M E, Ketit S, Prog. Org. Coat. **2001**, 43, 267.
[76] Labjar N, Lebrini M, Bentiss F, Chihib N E, El Hajjaji S, Jama C, acid, *Mater. Chem. Phys*. **2010**, 119, 330.
[77] Solmaz R, *Corros. Sci*. **2014**, 79, 169.
[78] Behpour M, Ghoreishi S M, Khayatkashani M, Soltani N, *Mater. Chem. Phys.* **2012**, 131, 621.
[79] Priya A R S, Muralidharam V S, Subramania A, *Corros.Sci*. **2008**, 64, 541.
[80] Macdonald J R, *Electroanal J. Chem*. **1987**, 223, 25.
[81] Mertens S F, Xhoffer C, De Cooman B C, Temmerman E, *Corros.Sci.* **1997**, 53, 381.
[82] Ergun U, Yuzer D, Emregul K C, *Mater. Chem. Phys*. **2008**, 109, 492.
[83] Qian B, Wang J, Zheng M, Hou B, *Corros. Sci*. **2013**, 75, 184.
[84] Moradi M, Duan J, Du X, *Corros. Sci*. **2013**, 69, 338.
[85] Stoynov Z B, Grafov B M, Savova-Stoynova B, Elkin V V, Electrochemical Impedance, Nauka, Moscow, **1991**.
[86] Growcock F B, Jasinski R I, *J. Electrochem. Soc.* **1989**, 136, 2310.
[87] Qu Q, Jiang S A, Bai W, Li L, *Electrochim. Acta* **2007**, 52, 6811.
[88] Musa A Y, Kadhum A A H, Mohamad A B, Takriff M S, *Corros. Sci.* **2010**, 52 3331.
[89] Li L, Zhang X, Lei J, He J, Zhang S, Pan F, *Corros. Sci.* **2012**, 63, 82.
[90] Goulart C M, Esteves-Souza A, Martinez-Huitle C A, Rodrigues C J F, Maciel M A M, Echevarria A, *Corros. Sci.* **2013,** 67, 281.
[91] Khaled K F, Jackerman N, *Electrochim. Acta.*, **2003**, 48, 2715.
[92] Ahamad I, Quraishi M A, *Corros. Sci*. **2009**, 51, 2006.
[93] Hegazy M A, Badawi A M, Abd El Rehim S S, Kamel W M, *Corros. Sci*. **2013**, 69, 110.
[94] Langmuir I, *Amer J. Chem. Soc*. **1947**, 39, 1848.
[95] Obot I B, Obi-Egbedi N O, Umoren S A, *Corros. Sci***. 2009**, 51, 1868.
[96] Aljourani J, Raeissi K, Golozar M A, *Corros. Sci.* **2009**, 51, 1836.
[97] Tourabi M, Nohair K, Traisnel M, Jama C, Bentiss F, *Corros. Sci*. **2013**, 75, 123.
[98] Keles H, Keles M, Dehri I, Serindag O, *Mater. Chem. Phys*. **2008**, 112, 173
[99] Keles H, Keles M, Dehri I, Serindag O, *Coll. Surf. A*., **2008**, 320, 138.
[100] Amin M A, Ibrahim M M, *Corros. Sci.* **2011**, 53, 873.
[101] Lebrini M, Robert F, Vezin H, Roos C, *Corros. Sci.* **2010**, 52, 3367.
[102] Bahrami M J, Hosseini S M A, Pilvar P, *Corros. Sci*. **2010**, 52, 2793.
[103] Solmaz R, *Corros. Sci.* **2014,** 81, 75.
[104] Ahamad I, Prasad R, Quraishi M A, *Corros. Sci*. **2010**, 52, 933.
[105] Lebrini M, Bentiss F, Vezin H, Lagrenée M, *Corros. Sci*. **2006**, 48, 1279.
[106] Hoar T P, Holliday R D, *J. Appl. Electrochem*. **1953**, 3, 502.
[107] Behpour M, Ghoreishi S M, Soltani N, Salavati-Niasari M, *Corros. Sci*. **2009,** 51, 1073.
[108] Vracˇar L M, Drazˇic D M, *Corros. Sci.* **2002,** 44, 1669.
[109] Lebrini M, Robert F, Vezin H, Roos C, *Corros. Sci*. **2010**, 52, 3367.
[110] Bahrami M J, Hosseini S M A, Pilvar P, *Corros. Sci*. **2010**, 52, 2793.
[111] Ozcan M, Solmaz R, Kardas G, Dehri I, *Coll. Surf.*, A **2008,** 325, 57.
[112] Abiola O K, Oforka N C, *Mater. Chem. Phys*. **2004**, 83, 315.
[113] Li X, Deng S, Fu H, *Corros. Sci.* 2011, 53, 302.
[114] El Mehdi B, Mernari B, Traisnel M, Bentiss F, Lagrenee M, *Mater. Chem. Phys*. **2002**, 77, 489.
[115] Popova A, Sokolova E, Raicheva S, Christov M, *Corros. Sci*. **2003**, 45, 33.
[116] Abd-El-Rehim S S, Refaey S A M, Taha F, Saleh M B, Ahmed R A, *J. Appl. Electrochem*. **2001**, 31, 429.
[117] Zhang J, Liu J, Yu W, Yan Y, You L, Liu L, *Corros. Sci*. **2010**, 52, 2059.
[118] Lebrini M, Lagrenee M, Traisnel M, Gengembre L, Vezin H, Bentiss F, *Appl. Surf. Sci.* **2007**, 253, 9267.
[119] Sastri V S, Perumareddi J R, *Corro. Sci*, **1997**, 53, 671.
[120] Pearson R G, *Inorg. Chem*. **1988**, 27, 734.
[121] Martinez S, *Mater. Chem. Phys*. **2002**, 77, 97.
[122] 122. Lukovits I, Kalman E, Zucchi F, *Corro. Sci***. 2001**, 57, 3.
[123] 123. Awad M K, Metwally M S, Soliman S A, El-Zomrawy A A, bedair M A. *J. Ind. Eng. Chem* **2013**, 42, 13.